



HAL
open science

Analysis of parity violation in chiral molecules.

Radovan Bast, Anton Koers, André Severo Pereira Gomes, Miroslav Iliáš,
Lucas Visscher, Peter Schwerdtfeger, Trond Saue

► **To cite this version:**

Radovan Bast, Anton Koers, André Severo Pereira Gomes, Miroslav Iliáš, Lucas Visscher, et al..
Analysis of parity violation in chiral molecules.. Physical Chemistry Chemical Physics, 2011, 13 (3),
pp.864-876. 10.1039/c0cp01483d . hal-00760960

HAL Id: hal-00760960

<https://hal.science/hal-00760960v1>

Submitted on 4 Nov 2021

HAL is a multi-disciplinary open access archive for the deposit and dissemination of scientific research documents, whether they are published or not. The documents may come from teaching and research institutions in France or abroad, or from public or private research centers.

L'archive ouverte pluridisciplinaire **HAL**, est destinée au dépôt et à la diffusion de documents scientifiques de niveau recherche, publiés ou non, émanant des établissements d'enseignement et de recherche français ou étrangers, des laboratoires publics ou privés.

Analysis of parity violation in chiral molecules

Radovan Bast,^a Anton Koers,^b André Severo Pereira Gomes,^c Miroslav Iliáš,^d Lucas Visscher,^b Peter Schwerdtfeger,^e and Trond Saue^{*f}

Received Xth XXXXXXXXXXXX 20XX, Accepted Xth XXXXXXXXXXXX 20XX

First published on the web Xth XXXXXXXXXXXX 200X

DOI: 10.1039/b000000x

In order to guide the experimental search for parity violation in molecular systems, in part motivated by the possible link to biomolecular homochirality, we present a detailed analysis in a relativistic framework of the mechanism behind the tiny energy difference between enantiomers induced by the weak force. A decomposition of the molecular expectation value into atomic contributions reveals that the effect can be thought of as arising from a *specific* mixing of valence $s_{1/2}$ and $p_{1/2}$ orbitals on a single center induced by a chiral molecular field. The intra-atomic nature of the effect is further illustrated by visualization of the electron chirality density and suggests that a simple model for parity violation in molecules may be constructed by combining pre-calculated atomic quantities with simple bonding models. A 2-component relativistic computational procedure is proposed which bridges the relativistic and non-relativistic approaches to the calculation of parity violation in chiral molecules and allows us to explore the single-center theorem in a variational setting.

1 Introduction

Emil Fischer's pioneering studies of peptides and sugars in 1891 led to the classification of chiral molecules,¹ (*D*)-sugars and (*L*)-amino acids in particular, and to the confirmation of Pasteur's original conjecture that the universe is dissymmetric². Note that chirality, or dissymmetry in the terminology of Pasteur,³ implies absence of improper rotations, that is, an achiral molecule is not necessarily devoid of any symmetry elements. The discovery that the basic molecular building blocks of living organisms have a distinct chirality, and that only one enantiomeric form ((*D*)-sugars and (*L*)-amino acids) is predominantly found in living systems, has puzzled researchers for more than a century.⁴ In fact, the study of proteinogenic amino acids from fossil bones shows that the (*L*)-form has been the exclusive component in life forms for at least 100 million years.⁵ It seems plausible that the onset

of biomolecular homochirality happened at an early stage in the chemical/biological evolution process on earth, perhaps around 4 billion years ago.

There are many hypotheses on the origin of biomolecular homochirality (an excellent review on the various hypotheses put forward over the last 60 years or so has been given by Bonner⁶). The hypotheses can be classified broadly into *biotic* and *abiotic* theories, with a further subdivision of abiotic theories into *deterministic* and *probabilistic*, and *terrestrial* and *extra-terrestrial* theories (panspermia theory for the latter).^{7–11} The field is heavily debated and open to much speculation, and it is fair to say that we do not have a clear understanding of the pre-biotic chemistry responsible for the emergence of single-handed molecules in life.¹² It is however clear that biomolecular homochirality is one (of the many) necessary conditions for life, as it is required to form the secondary, tertiary and quaternary structures of the proteins to function correctly, as well as the helical structure of the DNA and RNA. For example, Urata *et al.* showed that the incorporation of an (*L*)-ribonucleotide into the RNA or (*L*)-deoxyribonucleotide into the DNA strand leads to significant destabilization of the duplexes upsetting the Watson-Crick-pairing,¹³ and that the chirality of homochiral nucleic acids is the primary determinant for their helical sense.^{14,15} Moreover, this intrinsic chirality at the microscopic level leads to handedness at the macroscopic level.^{16,17}

A fundamental discovery in the middle of the last century is that electroweak interactions give rise to primarily left-spinning electrons during nuclear beta decay.¹⁸ This symmetry breaking originates from parity violation (PV) at the quantum level, correctly predicted in 1956 by Lee and Yang¹⁹

^a Centre for Theoretical and Computational Chemistry (CTCC), Department of Chemistry, University of Tromsø, N-9037 Tromsø, Norway. E-mail: radovan.bast@uit.no

^b Division of Theoretical Chemistry, Amsterdam Center for Multiscale Modeling, VU University – Faculty of Sciences, De Boelelaan 1083, NL-1081 HV Amsterdam, The Netherlands. E-mail: visscher@chem.vu.nl

^c Laboratoire PhLAM CNRS UMR 8523, Université de Lille 1, Bât P5, F-59655 Villeneuve d'Ascq Cedex, France. E-mail: aspgpp@gmail.com

^d Department of Chemistry, Faculty of Natural Sciences, Matej Bel University, Tajovského 40, 97400 Banská Bystrica, Slovakia. E-mail: ilias@fpv.umb.sk

^e Centre of Theoretical Chemistry and Physics (CTCP), The New Zealand Institute for Advanced Study (IAS), Massey University Auckland, Bldg.44, Private Bag 102904, North Shore City, 0745 Auckland, New Zealand. E-mail: p.a.schwerdtfeger@massey.ac.nz

^f Laboratoire de Chimie et Physique Quantiques (UMR 5626), CNRS and Université de Toulouse 3 (Paul Sabatier), 118 route de Narbonne, F-31062 Toulouse, France E-mail: trond.saue@irsamc.ups-tlse.fr

and put into a firm quantum theory by Weinberg, Salam and Glashow.^{20–23} Loosely speaking, our Universe is left-handed and mirror-image symmetry is broken in quantum processes, that is, the parity operator P does not commute anymore with the Hamiltonian of the system. This PV effect has been measured and calculated very accurately from electroweak theory for forbidden atomic transitions confirming the standard model in particle physics to high precision.^{24–27} From the standard model it is also accepted that PV can lead to a small energy difference between enantiomers of chiral molecules ($V_n - A_e$ coupling for the Z -boson exchange between electrons and the nucleons),^{28,29} although there is no experimental verification yet of this distinct symmetry breaking effect.^{30,31} For more recent reviews on PV effects in chiral molecules see refs. 32–35.

Yamagata suggested in 1966 that “The asymmetric appearance of biomolecules is most naturally explained by supposing a slight breakdown of parity in electromagnetic interaction and an accumulation of it in a series of chemical reactions”.³⁶ While this (perhaps over-enthusiastic) statement added a new hypothesis on the origin of biomolecular homochirality, his next statement “Conversely, it seems that the asymmetric existence of biomolecules verifies a parity non-conservation in electromagnetic interaction. ... This universality, if true, would promise similar results on other planets than the earth” is certainly incorrect. Note also that Yamagata discusses the possibility of parity violation in *electromagnetic* and not weak interactions. Nevertheless, the possibility that PV effects lead to a clear deterministic selection of one enantiomer over the other has led to an intense activity in this field, most notably in early days of electroweak quantum chemical investigations³⁷ by Mason and Tranter,^{38–43} and later by McDermott.^{44,45} However, the energy PV energy difference between the enantiomers is extremely small and on the order of 10^{-17} to 10^{-16} kJ mol⁻¹.^{46,47} Moreover, the preference for one enantiomer over the other critically depends on the conformation of the molecule and the interaction with other molecules (such as water). For instance, a slight rotation of the carboxyl group can easily change the energetic preference from an (*L*)-amino acid to the (*D*)-form.^{48–51} Moreover, as we learned in the last 10 years, the computational results are also critically dependent on the method applied.^{33,52–57} This led Bonner to the radical conclusion that “there is no causal connection whatsoever between parity violation in terrestrial biopolymers and that in nuclear processes, and that parity violation inherent in biopolymers is in no way the consequence of parity violation at the level of fundamental particles”.¹⁰ Nevertheless, PV as a cause of biomolecular homochirality cannot be strictly ruled out and requires more detailed investigations. What can perhaps be ruled out, though, is the Salam hypothesis of a PV initiated phase transition in (*D*)-amino acids, as large conversion barriers for the racemization in the solid state

would completely inhibit such a process.⁵⁸

In the last twenty years a number of research groups began to search for large PV effects in chiral molecules, both on the experimental and the theoretical side (e.g. see review articles^{33–35,47,59–61} on this subject). Yet, we are currently not in the position to design new chiral molecules and estimate PV effects by its order of magnitude without resorting to calculations. All we currently rely on is the high Z -scaling rule for the nuclear spin-independent and the nuclear spin-dependent components of the electroweak perturbation.^{28,29,37,62–64} A deeper understanding of the mechanisms of PV in molecular systems is very much needed in order to better guide experiment. A significant contribution was provided by Hegstrom, Rein and Sandars³⁷, pointing out the connection to optical activity in molecules and introducing the single-center theorem. A qualitative model of the PV in molecular systems was proposed by Faglioni and Lazzeretti in a non-relativistic framework⁶⁵. In the present work we present a detailed analysis of PV in chiral molecules, but now in a 4-component relativistic framework, which we believe will help to assist further investigations in this new emerging field. In particular, we perform a decomposition of the molecular expectation value in intra- and inter-atomic contributions as well as a visualization of the electron chirality density.^{66,67} We furthermore propose a bridge between the relativistic and non-relativistic approaches to the calculation of the PV energy in molecules by exploring the single-center theorem³⁷ in a variational setting.

2 Theory

2.1 Parity violation energy in molecular systems

The parity violating weak interaction in molecules is dominated by the exchange of Z^0 bosons between electrons and nuclei (quarks). Detailed discussions of the interaction Hamiltonian relevant for the study of PV in atoms and molecules are found in refs. 32,53,68–70. In the following we shall simply sketch a derivation highlighting differences between the weak and the electromagnetic interaction.

The Hamiltonian describing electromagnetic interactions may be expressed as⁷¹

$$H_{\text{int}}^{\text{em}} = - \int j_{\mu} A_{\mu} d\tau, \quad (1)$$

where appears the 4-current $j_{\mu} = (\mathbf{j}, ic\rho)$ and 4-potential $A_{\mu} = (\mathbf{A}, i\phi/c)$. In the following we employ implicit summation and, following Sakurai,⁷² express 4-vectors using imaginary i rather than resorting to a metric. The 4-potential is the solution of Maxwell’s equation which in Lorentz gauge reads

$$\square^2 A_{\mu} = -4\pi(j_{\mu}/c^2), \quad (2)$$

where appears the d'Alembertian $\square^2 = \nabla^2 - \frac{1}{c^2} \frac{\partial^2}{\partial t^2}$. Here and in the following we employ SI-based atomic units. The electromagnetic interaction is mediated by photons. Anticipating massive vector bosons, we generalize the corresponding equation for the Green's function (propagator) as

$$(\square^2 - M^2 c^2) G(\mathbf{r}, t; \mathbf{r}', t') = -4\pi\delta(\mathbf{r} - \mathbf{r}') \quad (3)$$

which corresponds to the Klein-Gordon equation with a source term. The 4D Fourier transformed Green's function is given by

$$G(\mathbf{k}, \omega) = \frac{4\pi}{p_\mu p_\mu + M^2 c^2}; \quad p_\mu = (\mathbf{k}, i\omega/c). \quad (4)$$

Two limiting cases may now be distinguished: In the case of electromagnetic interactions, the vector bosons (photons) do not carry mass, and the (retarded) Green's function simplifies to

$$G^{(+)}(\mathbf{r}, t; \mathbf{r}', t') = \frac{\delta(t' - t_r)}{|\mathbf{r} - \mathbf{r}'|}; \quad t_r = t - \frac{|\mathbf{r} - \mathbf{r}'|}{c}. \quad (5)$$

The electromagnetic interaction Hamiltonian eqn (1) can thus be expressed as

$$H_{\text{int}}^{\text{em}} = -\frac{1}{c^2} \int \frac{j_\mu(\mathbf{r}, t) j_\mu(\mathbf{r}', t_r)}{|\mathbf{r} - \mathbf{r}'|} d\tau d\tau'. \quad (6)$$

In the second limiting case the mass of the vector boson overwhelms momentum exchange ($p_\mu p_\mu$) which leads to an interaction Hamiltonian on the contact form given by Fermi in his explanation of β -decay in 1934⁷³ (see ref. 74 for an English translation). An effective Hamiltonian for the weak interaction between electrons and nucleons, mediated by the neutral and massive Z^0 boson is accordingly given by

$$H_{\text{int}}^{\text{Fermi}} = \frac{4\pi}{M_Z^2 c^4} \int j_\mu^e(\mathbf{r}, t) \left(\sum_i^Z j_{\mu,i}^p(\mathbf{r}, t) + \sum_i^N j_{\mu,i}^n(\mathbf{r}, t) \right) d\tau. \quad (7)$$

The mass of the Z^0 boson is 91.1876(21) GeV/c²,⁷⁵ that is, close to 98 Da.

Intriguingly, the weak force is the only interaction mediated by massive vector bosons, leading to a contact-like interaction, and also the only interaction allowing PV (the short range of the nuclear force, despite the strong interaction being mediated by massless gluons, is due to its van der Waals like character⁶⁹). The electromagnetic currents are vector quantities

$$j_\mu = -ec\psi^\dagger(\boldsymbol{\alpha}, i)\psi, \quad (8)$$

meaning that the spatial component changes sign under inversion. They combine, however, to give a parity conserving interaction. In contrast, the neutral currents of the weak interaction are combinations of vector and axial-vector forms

$$j_\mu = \frac{ec}{2\sin(2\theta_W)} \left[\underbrace{C_V \psi^\dagger(\boldsymbol{\alpha}, i)\psi}_{(-,+)} - C_A \psi^\dagger(\boldsymbol{\Sigma}, i\gamma_5)\psi \right], \quad (9)$$

where appears the γ_5 matrix

$$\gamma_5 = \begin{bmatrix} 0_2 & 1_2 \\ 1_2 & 0_2 \end{bmatrix} \quad (10)$$

and the Weinberg angle θ_W which describes the rotation of B^0 and W^0 bosons by spontaneous symmetry breaking to form photons and Z^0 bosons. The most recent value⁷⁶ is $\sin^2 \theta_W = 0.2397(13)$ (in the present work we have employed $\sin^2 \theta_W = 0.2319$). The axial-vector coupling coefficients for the neutron, proton and electron are $C_A^n = -C_A^p = C_A^e = -1$, respectively. Likewise, the vector coupling coefficients are $C_V^n = -1$ and $C_V^p = -C_V^e = 1 - 4\sin^2 \theta_W$. For the nucleon currents a non-relativistic approximation is employed,⁷⁰ setting the small components to zero, such that only parity conserving parts of the currents are retained.

The parentheses below the underbraces in eqn (9) indicate the behaviour of the space and time components under inversion. Combining the space components of the nucleon axial-vector currents and the electron vector current and ($A_n - V_e$ coupling) leads to a nuclear spin-dependent interaction Hamiltonian which has been employed in theoretical studies of PV in NMR spectra^{64,77-87}. In the present work, however, we focus exclusively on the PV nuclear spin-independent interaction Hamiltonian which is obtained by combining the time components of the nucleon vector currents and the electron axial-vector current ($V_n - A_e$ coupling). At the 4-component relativistic level it is given by

$$H_{\text{PV}} = \sum_A H_{\text{PV}}^A; \quad H_{\text{PV}}^A = \frac{G_F}{2\sqrt{2}} Q_w^A \sum_i \gamma_5(i) \rho^A(\mathbf{r}_i), \quad (11)$$

in which appears the weak nuclear charge

$$Q_w^A = Z^A C_V^p + N^A C_V^n = Z^A (1 - 4\sin^2 \theta_W) - N^A \quad (12)$$

with Z^A and N^A representing the number of protons and neutrons in nucleus A . The presence of normalized nuclear charge densities ρ^A restricts integration over electron coordinates \mathbf{r}_i to nuclear regions and thereby provides a natural partitioning of the operator in atomic contributions \hat{H}_{PV}^A . The Fermi coupling constant

$$G_F = 2.22255 \times 10^{-14} E_h a_0^3 \approx 2\sqrt{2} \left(\frac{4\pi\hbar^2}{4\pi\epsilon_0 M_Z^2 c^4} \right) \left(\frac{ec}{2\sin(2\theta_W)} \right)^2 \quad (13)$$

implies that the interaction is truly weak (the right-hand side formula is only approximate in that the cited value also contains radiative corrections). The parity violating energy E_{PV} can accordingly not be simply extracted from the total electronic energy of a molecule in standard floating point calculations and should rather be obtained in the framework of perturbation theory. In a relativistic framework the parity violating energy can be calculated as an expectation value

$$E_{\text{PV}} = \sum_A \langle H_{\text{PV}}^A \rangle. \quad (14)$$

In a non-relativistic (NR) framework the PV Hamiltonian reduces to

$$H_{\text{PV};\text{NR}} = \sum_A H_{\text{PV};\text{NR}}^A; \quad H_{\text{PV};\text{NR}}^A = \frac{G_{\text{F}}}{4mc\sqrt{2}} Q_{\text{w}}^A \sum_i \{ \boldsymbol{\sigma}_i \cdot \mathbf{p}, \rho^A(\mathbf{r}_i) \}_{+}. \quad (15)$$

This purely imaginary operator gives zero expectation value for NR (real) wave functions. In a NR framework the parity violating energy is therefore calculated as a static linear response function^{52,54}

$$E_{\text{PV};\text{NR}} = \sum_{AB} \langle \langle H_{\text{PV};\text{NR}}^A; H_{\text{SO}}^B \rangle \rangle_0 \quad (16)$$

(or approximated by a sum-over-states expression) by coupling the NR PV operator with an operator describing spin-orbit (SO) coupling contributions from individual centers. A Z_A^5 scaling law has been deduced for E_{PV}^A in molecular systems, based on both the relativistic,²⁸ eqn (14), and NR^{29,37,62} expressions, eqn (16), for the PV energy.

2.2 Projection analysis of expectation values

At the 4-component relativistic Hartree–Fock (HF) and Kohn–Sham (KS) level of theory the PV energy E_{PV} is straightforwardly calculated as an expectation value. Further insight can be obtained by subjecting the expectation value to projection analysis. Consider the expectation value of some operator $\hat{\Omega}$ in the HF or KS approach

$$\Omega = \langle \Psi | \hat{\Omega} | \Psi \rangle = \sum_i^{N_{\text{occ}}} \langle \psi_i | \hat{\Omega} | \psi_i \rangle. \quad (17)$$

We proceed, in the spirit of for instance the Townes–Dailey model for nuclear quadrupole coupling constants,⁸⁸ by expanding the molecular orbitals (MO) ψ_i in the atomic orbitals ψ_j^A of the constituent atoms

$$|\psi_i\rangle = \sum_{Aj} |\psi_j^A\rangle c_{ji}^A + |\psi_i^{\text{pol}}\rangle, \quad (18)$$

where the index A labels the individual atoms (or, more generally, individual fragments). Typically only the occupied fragment orbitals will be employed, so whatever part of the molecular orbitals which is not spanned by the selected set of fragment orbitals is denoted the polarization contribution ψ_i^{pol} , which by construction is orthogonal to the fragment orbitals. Projecting eqn (18) from the left by any fragment orbital ψ_k^B gives a system of linear equations

$$\sum_{Aj} \langle \psi_k^B | \psi_j^A \rangle c_{ji}^A = \langle \psi_k^B | \psi_i \rangle, \quad (19)$$

which determines the expansion coefficients c_{ji}^A .

Inserting the MO expansion, eqn (18) into the expectation value, eqn (17) we obtain several terms

$$\begin{aligned} \langle \Psi | \hat{\Omega} | \Psi \rangle &= \underbrace{\sum_A \sum_{ijk} \langle \psi_i^A | \hat{\Omega} | \psi_j^A \rangle c_{ik}^{A*} c_{jk}^A}_{\text{intra-atomic}} \\ &+ \underbrace{\sum_{A \neq B} \sum_{ijk} \langle \psi_i^A | \hat{\Omega} | \psi_j^B \rangle c_{ik}^{A*} c_{jk}^B}_{\text{inter-atomic}} \\ &+ (\text{pol}), \end{aligned} \quad (20)$$

which are conveniently divided into three classes: i) intra-atomic contributions involve only atomic orbitals from the same center, ii) inter-atomic contributions involve atomic orbitals from two centers and iii) polarization contributions involve ψ_i^{pol} . The usefulness of the projection analysis deteriorates with increasing importance of the latter contributions, since they blur the distinction between intra- and inter-atomic contributions. Setting $\hat{\Omega}$ to the identity operator gives the starting point for a population analysis⁸⁹ equivalent to that of Mulliken, but cured of the strong basis-set dependence which renders Mulliken population analysis at best ambiguous in many cases.

3 Computational details

All calculations have been carried out with a development version of the DIRAC program package.⁹⁰ For the series H_2X_2 ($X = \text{O}, \text{S}, \text{Se}, \text{Te}, \text{Po}$) we have carried out 4-component relativistic HF and KS calculations based on the Dirac–Coulomb (DC) Hamiltonian. We have employed the density functionals LDA (SVWN5),^{91,92} BLYP,^{93–95} and B3LYP,^{96,97} representative of the three first rungs of the Jacob’s ladder of density functional approximations.⁹⁸ We have adopted the even-tempered basis sets and geometric parameters of ref. 63 with the H–X–X–H dihedral angle defined to correspond to the (*P*)-enantiomer. The small component basis sets were generated by restricted kinetic balance imposed in the canonical orthonormalization step.⁹⁹ The two-electron Coulomb integrals (SS|SS), involving only the small components, were neglected in all calculations and the energy corrected by a simple point-charge model.¹⁰⁰ For the projection analysis atomic orbitals for the constituent atoms were precalculated in their own atomic basis based on the ground state electronic configurations. We employed average SCF in the case of HF and fractional occupation in the case of KS.

For the CHBrClF molecule we carried out 4- and 2-component relativistic HF calculations, the latter based on the one-step, exact two-component (X2C) relativistic Hamiltonian¹⁰¹ in spin–orbit free form. We employed the AMFI code^{102,103} to provide one- and two-electron spin–orbit cor-

rections, see ref. 104 for more details. For comparative purposes with respect to the 4-component DC Hamiltonian, the two-electron SO terms of the AMFI operator contain only the spin-same-orbit part. A specificity of our interface to AMFI is that it allows the selection of nuclei for which spin-orbit corrections are supplied. Basis sets and geometric parameters as well as the scalar relativistic CCSD(T) potential curve along the C–F stretching mode were taken from ref. 105. The PV shift was calculated by double perturbation theory⁵⁶

$$\Delta P_{0 \rightarrow 1} = 2(P_1 - P_0) \approx \frac{\hbar}{\mu\omega_e} \left[P^{[2]} - \frac{1}{\mu\omega_e^2} P^{[1]} V^{[3]} \right] \quad (21)$$

where $V^{[n]}$ and $P^{[n]}$ are the MacLaurin expansion coefficients of the potential and property curves along the normal coordinate q , respectively. $P_n = \langle n|P(q)|n \rangle$ is the value of the property, in this case E_{PV} , in vibrational state n of the selected normal mode and μ is the corresponding reduced mass.

Unless otherwise stated, a Gaussian charge distribution has been chosen as the nuclear model using the recommended values of ref. 106. All basis sets are used in the uncontracted form.

4 Results and discussion

4.1 Projection analysis of the PV expectation value

The PV energy can be written as a sum of atomic contributions

$$E_{PV} = \sum_A E_{PV}^A = \frac{G_F}{2\sqrt{2}} \sum_A Q_w^A M_{PV}^A. \quad (22)$$

In the following we will concentrate on the reduced contributions $M_{PV}^X = \langle \Psi | \gamma_5 \rho^X | \Psi \rangle$. In Figure 1 we show the reduced contribution M_{PV}^{Te} of a Te atom in H_2Te_2 as a function of the H–Te–Te–H dihedral angle φ , calculated at the HF level as well as with three different density functionals. We observe the characteristic sigmoidal curve found for H_2X_2 systems by previous authors^{40,52,53,55,63,64,83,107,108} and which is also found when optical activity is plotted as a function of dihedral angle for the same systems (see for instance ref. 109). The M_{PV}^X is zero by symmetry for dihedral angles 0° and 180° , whereas the crossing of the abscissa in the vicinity of dihedral angle 90° occurs for a chiral conformation and therefore bars the use of the PV energy E_{PV} as a chirality measure, as is the case for any pseudoscalar function.^{110,111} We note that the four curves traced in Figure 1 are qualitatively the same, but the three density functionals distinguish themselves from HF by giving more pronounced maxima around 45° and minima around 135° .

A compact representation of the sigmoidal curves is provided by Fourier decomposition

$$M_{PV}^X(\varphi) = \sum_{n=1}^{\infty} F_n^X \sin(n\varphi). \quad (23)$$

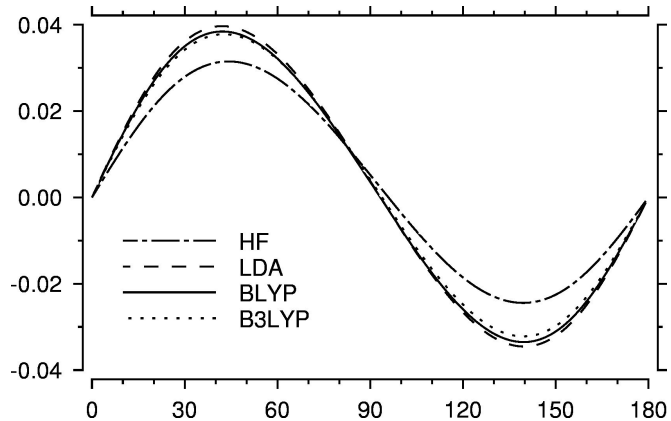


Fig. 1 Reduced contribution M_{PV}^{Te} for H_2Te_2 as a function of dihedral angle. All values in atomic units

In Figure 2 we trace the Fourier components of the reduced contribution M_{PV}^{Te} of a Te atom in H_2Te_2 as a function of dihedral angle φ , calculated at the HF level. The curve is clearly dominated by the F_2 component, whereas the F_1 is the prime responsible for shifting the crossing of the abscissa off from dihedral angle 90° . In Table 1 we give the F_2 component of M_{PV}^X for the series H_2X_2 ($X = \text{O}, \text{S}, \text{Se}, \text{Te}, \text{Po}$). One clearly sees how the values obtained with the three density functionals LDA, BLYP and B3LYP tend to cluster away from the HF value, although the distinction becomes less pronounced for the heavier systems. One also observes that the PV energy increases by orders of magnitude for the heavier systems. We will explore the scaling of the PV energy in more detail later in this section.

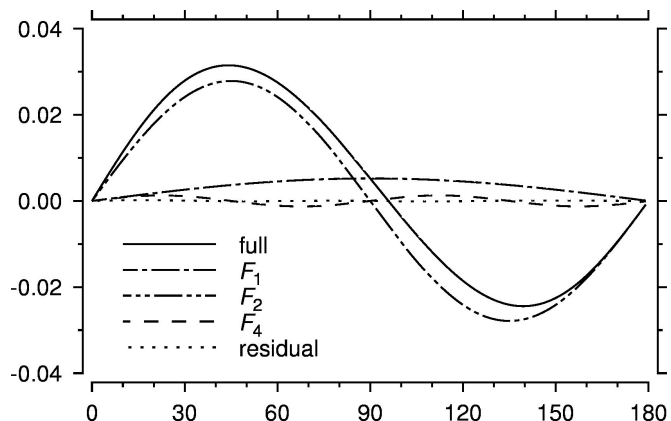


Fig. 2 Fourier decomposition of the reduced contribution M_{PV}^{Te} for H_2Te_2 calculated at the HF level as a function of dihedral angle. All values in atomic units.

Table 1 Fourier component F_2 of the reduced contribution M_{PV}^X to the PV energy for the series H_2X_2 ($X = \text{O}, \text{S}, \text{Se}, \text{Te}, \text{Po}$). All values in atomic units. The square brackets denote powers of 10

	H_2O_2	H_2S_2	H_2Se_2	H_2Te_2	H_2Po_2
HF	6.729[-6]	7.435[-5]	3.163[-3]	2.787[-2]	7.955[-1]
LDA	7.441[-6]	9.522[-5]	4.335[-3]	3.697[-2]	7.444[-1]
BLYP	7.238[-6]	9.554[-5]	4.204[-3]	3.585[-2]	7.504[-1]
B3LYP	7.163[-6]	9.162[-5]	4.055[-3]	3.488[-2]	7.703[-1]

In order to obtain a deeper understanding of parity violation in molecular systems, we will subject the reduced contributions M_{PV}^X to the projection analysis of expectation values introduced in section 2.2. Our results are summarized in Tab. 2 and illustrated for H_2Te_2 in Figure 3. All numbers refer to HF calculations, but the conclusions are valid for the KS level as well. The projection analysis clearly shows that the reduced contribution M_{PV}^X is completely dominated by intra-atomic contributions from the same center (X), although some uncertainty is introduced by the polarization contribution, which rises rather steadily from 4.7% to 20.3% through the series. All other intra-atomic contributions as well as the inter-atomic contributions are completely negligible. For H_2Po_2 we find that the inclusion of the virtual $7s_{1/2}$ orbital in the projection analysis reduces the polarization contribution from 20.3% to below 6.0%. We believe that this is due to the combined effect of the increasing polarisability of atoms when descending a row in the periodic table and the significant relativistic stabilization of the $7s_{1/2}$ orbital. We find, though, that the contribution of the $7s_{1/2}$ orbital to the electronic configuration of the polonium atom in the molecule is negligible.

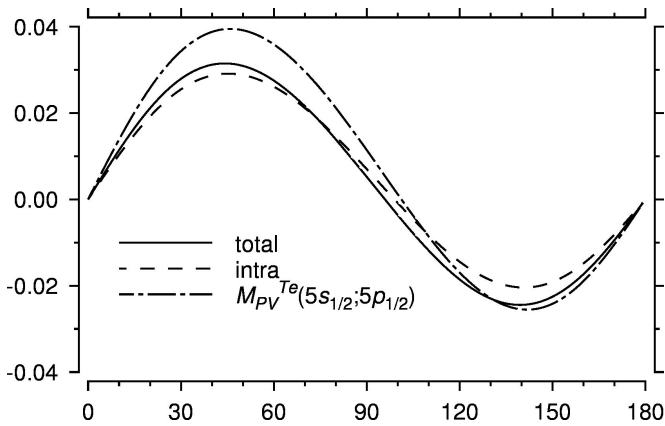


Fig. 3 Projection analysis of the reduced contribution $M_{\text{PV}}^{\text{Te}}$ for H_2Te_2 calculated at the HF level as a function of dihedral angle, see text for more details. All values in atomic units.

The atomic nature of the reduced contribution M_{PV}^X allows us to deepen the analysis by expressing it in terms of atomic

orbitals from the same center X . We write the 4-component relativistic atomic orbitals as

$$\Psi = \begin{bmatrix} \Psi^{L\alpha} \\ \Psi^{L\beta} \\ \Psi^{S\alpha} \\ \Psi^{S\beta} \end{bmatrix} = \begin{bmatrix} R^L(r)\chi_{\kappa,m_j}(\theta,\phi) \\ iR^S(r)\chi_{-\kappa,m_j}(\theta,\phi) \end{bmatrix}, \quad (24)$$

where R^L and R^S are the large and small radial functions, respectively and χ_{κ,m_j} the 2-component angular functions. Our analysis so far shows that M_{PV}^X is very well approximated by

$$\begin{aligned} M_{\text{PV}}^X &\approx \sum_{ij} \langle \Psi_i^X | \gamma_5 \rho^X | \Psi_j^X \rangle \\ &= i \left\{ \langle R_i^{L;X} | \rho^X | R_j^{S;X} \rangle_r \langle \chi_{\kappa_i,m_i}^X | \chi_{-\kappa_j,-m_j}^X \rangle_{\theta,\phi} \right. \\ &\quad \left. - \langle R_i^{S;X} | \rho^X | R_j^{L;X} \rangle_r \langle \chi_{-\kappa_i,m_i}^X | \chi_{\kappa_j,-m_j}^X \rangle_{\theta,\phi} \right\}, \quad (25) \end{aligned}$$

where subscripts r and (θ, ϕ) refer to radial and angular integration, respectively. From the angular integration we obtain the restrictions $\kappa_i = -\kappa_j$ and $m_i = m_j$. These already imply that the expectation value is strictly zero for an unpolarized atom. Further insight is obtained from the radial integration. Due to the extremely local nature of the nuclear charge distribution, it is sufficient to consider small r solutions of the radial functions^{112,113}

$$R^L = r^{\gamma-1}(p_0 + p_1 r + p_2 r^2 + \dots) \quad (26)$$

$$R^S = r^{\gamma-1}(q_0 + q_1 r + q_2 r^2 + \dots). \quad (27)$$

For a point nucleus $\gamma = +\sqrt{\kappa^2 - Z^2/c^2} < |\kappa|$ such that there is a weak singularity at the nucleus for $|\kappa| = 1$. This implies that the only contributions to M_{PV}^X arises from the mixing of $s_{1/2}$ and $p_{1/2}$ orbitals on the same center X . However, further contributions are allowed if we consider the more realistic model of extended nuclei. We then have $\gamma = |\kappa|$ and no singularities. For $\kappa < 0$ we have $q_0 = p_1 = 0$, whereas for $\kappa > 0$ the conditions $p_0 = q_1 = 0$ hold. Again only $s_{1/2}$ and $p_{1/2}$ orbitals have non-zero contributions at the origin. In particular, for $s_{1/2}$ orbitals $R^L = p_0$ and $R^S = 0$, where p_0 is determined from the normalization of the orbital. Likewise, for $p_{1/2}$ orbitals

Table 2 Summary of projection analysis of the reduced contribution M_{PV}^X to the PV energy, calculated at the HF level, for the series H_2X_2 ($X = \text{O}, \text{S}, \text{Se}, \text{Te}, \text{Po}$). All values in atomic units. The square brackets denote powers of 10

	H_2O_2	H_2S_2	H_2Se_2	H_2Te_2	H_2Po_2
full	6.492[-6]	7.435[-5]	3.163[-3]	2.787[-2]	7.955[-1]
intra(X)	5.879[-6]	6.876[-5]	2.717[-3]	2.459[-2]	6.334[-1]
inter	3.060[-7]	-1.212[-6]	3.074[-5]	-1.233[-4]	9.569[-4]
polar	3.066[-7]	6.798[-6]	4.152[-4]	3.407[-3]	1.611[-1]
$M_{\text{PV}}^X(ns_{1/2}; np_{1/2})$	8.819[-6]	8.548[-5]	3.773[-3]	3.216[-2]	7.728[-1]

$R^L = 0$ and $R^S = q_0$ where q_0 is determined from normalization. However, the finite extent of the nuclear charge distribution means that contributions from any pair of atomic orbitals with same j , but opposite κ is now allowed. These findings are illustrated in Tables 3 and 4 where we give selected matrix elements $\langle \Psi_i^{\text{Po}} | \gamma_5 \rho^{\text{Po}} | \Psi_j^{\text{Po}} \rangle$ for the polonium atom using a Gaussian and a point charge nuclear model. In Table 3 such elements are given between $s_{1/2}$ and $p_{1/2}$ orbitals. It can be seen that the difference between the values of the matrix elements obtained with the two different models for the nuclear charge distribution are rather small. One can also observe a difference of orders of magnitude of such matrix elements when going from core to valence orbitals. In Table 4 such elements are given between $p_{3/2}$ and $d_{3/2}$ orbitals. With a point nucleus such matrix elements are indeed zero (to machine precision), whereas non-zero values are found with an extended (Gaussian) nucleus, albeit significantly smaller than the matrix elements involving $s_{1/2}$ and $p_{1/2}$. Although Kriplovich¹¹⁴ points out that a finite nucleus does result in mixing of orbitals other than $s_{1/2}$ and $p_{1/2}$, we are not aware of studies of atomic PV that explore the modification of selection rules by the combination of PV and the finite size of the nucleus demonstrated above.

The picture that emerges from our analysis so far is that the PV energy arises from mixing of atomic orbitals, in particular $s_{1/2}$ and $p_{1/2}$ in the presence of a chiral molecular field. This is in line with previous theoretical considerations^{37,40,68,114,115}. The novelty of our approach is that we have developed an analysis tool which allows us to study these effects in a detailed and quantitative manner for any molecular system.

In atoms such mixing leads to non-zero transition amplitudes for parity-forbidden electric dipole transitions such as the $6S_{1/2} \rightarrow 7S_{1/2}$ transition in cesium which has been observed by experiment.^{116,117} Clearly $s_{1/2}$ and $p_{1/2}$ orbitals already mix in the X_2 moiety for which E_{PV} is strictly zero, so the *nature* of this mixing has to be considered in more detail. We note that according to eqn (25) the inter-atomic matrix elements $\langle \Psi_i^X | \gamma_5 \rho^X | \Psi_j^X \rangle$ should be purely imaginary, whereas the

actual elements given in Tables 3 and 4 are real. This follows from a specific choice of phase, which will be important in the following. Relativistic atomic orbitals are usually given as in eqn (24) with a purely imaginary phase on the small component to assure real radial functions, but this is not the only possibility. We will introduce a choice of phase that to largest possible extent leads to real coefficients when mixing atomic orbitals into molecular ones. 4-component relativistic orbitals (4-spinors) span fermion irreps, that is, the extra irreps of the double groups. However, as pointed out in ref. 118, the real and imaginary parts of each component span boson irreps, that is, the irreps of single point groups. The phase of atomic orbitals is fixed to within a real phase by insisting on a specific symmetry structure of *gerade* and *ungerade* orbitals

$$\Psi_g = \begin{bmatrix} (\Gamma_0, \Gamma_{R_z}) \\ (\Gamma_{R_y}, \Gamma_{R_x}) \\ (\Gamma_{xyz}, \Gamma_z) \\ (\Gamma_y, \Gamma_x) \end{bmatrix}; \quad \Psi_u = \begin{bmatrix} (\Gamma_{xyz}, \Gamma_z) \\ (\Gamma_y, \Gamma_x) \\ (\Gamma_0, \Gamma_{R_z}) \\ (\Gamma_{R_y}, \Gamma_{R_x}) \end{bmatrix} = \Gamma_{xyz} \otimes \Psi_g. \quad (28)$$

In the above expression Γ_0 refers to the totally symmetric irrep, Γ_q and Γ_{R_q} ($q = x, y, z$) to the symmetry of the coordinates and rotations, respectively, and finally Γ_{xyz} to the symmetry of the function xyz , which is the symmetry of the γ_5 matrix. In fact, the phases are fixed by selecting Γ_0 and Γ_{xyz} for *gerade* and *ungerade* orbitals, respectively, as the symmetry of the real part of the $L\alpha$ component. With this choice of phase, $s_{1/2}$ will have the structure as given in eqn (24), but for $p_{1/2}$ orbitals the imaginary phase is moved to the *large* component. The matrix elements between $s_{1/2}$ and $p_{1/2}$ orbitals now become purely real, that is,

$$\langle s_{1/2}^X | \gamma_5 \rho^X | p_{1/2}^X \rangle = \langle R_s^{L:X} | \rho^X | R_p^{S:X} \rangle_r + \langle R_s^{S:X} | \rho^X | R_p^{L:X} \rangle_r. \quad (29)$$

Consider now the mixing of $s_{1/2}$ and $p_{1/2}$ orbitals on the same center X when atomic symmetry is broken in a molecule

$$\begin{bmatrix} \Psi_+ \\ \Psi_- \end{bmatrix} = \begin{bmatrix} \cos \theta & e^{i\phi} \sin \theta \\ -e^{-i\phi} \sin \theta & \cos \theta \end{bmatrix} \begin{bmatrix} s_{1/2}^X \\ p_{1/2}^X \end{bmatrix}; \quad \theta \in \left[-\frac{\pi}{2}, \frac{\pi}{2} \right]. \quad (30)$$

The generally unitary transformation has been selected such that the resulting function Ψ_+ has a real coefficient $\cos \theta$ for

Table 3 Matrix elements $\langle \psi_i^{\text{Po}} | \gamma_5 \rho^{\text{Po}} | \psi_j^{\text{Po}} \rangle$ between $s_{1/2}$ and $p_{1/2}$ orbitals, calculated at the HF level. Numbers are given for a Gaussian nuclear model as well as a point nucleus model, the latter in parenthesis. All values in atomic units. The square brackets denote powers of 10

	$2p_{1/2}$	$3p_{1/2}$	$4p_{1/2}$	$5p_{1/2}$	$6p_{1/2}$
$1s_{1/2}$	1.385[+5] (1.551[+5])	-7.082[+4] (-7.942[+4])	3.583[+4] (4.018[+4])	1.573[+4] (1.764[+4])	-4.904[+3] (-5.499[+3])
$2s_{1/2}$	5.486[+4] (6.148[+4])	-2.806[+4] (-3.148[+4])	1.419[+4] (1.593[+4])	6.233[+3] (6.992[+3])	-1.943[+3] (-2.180[+3])
$3s_{1/2}$	-2.646[+4] (-2.966[+4])	1.354[+4] (1.519[+4])	-6.847[+3] (-7.683[+3])	-3.007[+3] (-3.373[+3])	9.372[+2] (1.051[+3])
$4s_{1/2}$	1.345[+4] (1.508[+4])	-6.881[+3] (-7.720[+3])	3.481[+3] (3.906[+3])	1.529[+3] (1.715[+3])	-4.765[+2] (-5.346[+2])
$5s_{1/2}$	-6.182[+3] (-6.929[+3])	3.162[+3] (3.548[+3])	-1.600[+3] (-1.795[+3])	-7.024[+2] (-7.881[+2])	2.190[+2] (2.457[+2])
$6s_{1/2}$	2.260[+3] (2.534[+3])	-1.156[+3] (-1.297[+3])	5.849[+2] (6.562[+2])	2.568[+2] (2.881[+2])	-8.006[+1] (-8.982[+1])

Table 4 Matrix elements $\langle \psi_i^{\text{Po}} | \gamma_5 \rho^{\text{Po}} | \psi_j^{\text{Po}} \rangle$ between $p_{3/2}$ and $d_{3/2}$ orbitals, calculated at the HF level. Numbers are given for a Gaussian nuclear model as well as a point nucleus model, the latter in parenthesis. All values in atomic units. The square brackets denote powers of 10

	$3d_{3/2}$	$4d_{3/2}$	$5d_{3/2}$
$2p_{3/2}$	-1.185[-02] (-4.598[-21])	6.311[-03] (2.403[-22])	-2.348[-03] (4.869[-20])
$3p_{3/2}$	6.277[-03] (-2.365[-20])	-3.343[-03] (1.236[-21])	1.244[-03] (2.504[-19])
$4p_{3/2}$	-3.193[-03] (1.052[-20])	1.701[-03] (-5.500[-22])	-6.330[-04] (-1.114[-19])
$5p_{3/2}$	1.380[-03] (-2.491[-19])	-7.348[-04] (1.302[-20])	2.734[-04] (2.638[-18])
$6p_{3/2}$	3.989[-04] (3.287[-19])	-2.125[-04] (-1.718[-20])	7.907[-05] (-3.480[-18])

the $s_{1/2}$ orbital. We then find

$$\begin{aligned} \langle \psi_+ | \gamma_5 \rho^X | \psi_+ \rangle &= 2 \cos \theta \cos \phi \sin \theta \langle s_{1/2}^X | \gamma_5 \rho^X | p_{1/2}^X \rangle \\ &= -\langle \psi_- | \gamma_5 \rho^X | \psi_- \rangle. \end{aligned} \quad (31)$$

From the above result we can draw two conclusions: i) The presence of the factor $\cos \phi$ in the above expression shows that a non-zero contribution is only obtained when the mixing coefficient of the $p_{1/2}$ orbital has a *real* component. ii) ψ_+ and ψ_- must contribute with unequal weight in the molecular wave function, otherwise they cancel each other. The latter conclusion explains why core orbitals generally do not contribute to the PV energy,⁶³ although Tables 3 and 4 show that their matrix elements are significantly larger than matrix elements over valence orbitals. Indeed, Figure 3 and Table 2 clearly show that the reduced contribution M_{PV}^X is completely dominated by the mixing of *valence* $s_{1/2}$ and $p_{1/2}$ orbitals on the same center X .

The above analysis shows that for the series H_2X_2 ($X = \text{O}, \text{S}, \text{Se}, \text{Te}, \text{Po}$) the reduced contribution is very well approximated

by

$$M_{\text{PV}}^X \approx \underbrace{\langle ns_{1/2}^X | \gamma_5 \rho^X | np_{1/2}^X \rangle}_{\text{“total”}} 2\text{Re} \overbrace{\left[\sum_i c(ns_{1/2}^A)_i^* c(np_{1/2}^A)_i \right]}^{\text{“mixing”}}, \quad (32)$$

where the index i sums over molecular orbitals. In Figure 4 we give a log-log plot showing the scaling behaviour of the reduced contribution along the series. Although not strictly linear, it can be seen that the atomic matrix element $\langle ns_{1/2}^X | \gamma_5 \rho^X | np_{1/2}^X \rangle$ scales approximately as $Z^{2.6}$, thus confirming the Z^3 scaling law proposed by Bouchiat and Bouchiat⁶⁸. The mixing coefficient, which we from eqn (16) can associate with spin-orbit coupling from the neighbouring centers, scales as $Z^{2.1}$, thus giving an overall scaling $Z^{4.8}$, in agreement with previous estimates.^{28,29,37,62}

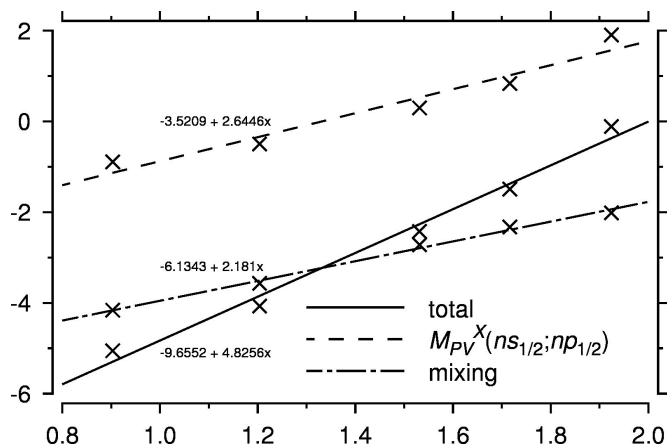


Fig. 4 Log-log plot showing the scaling of reduced contribution M_{PV}^X as a function of nuclear charge Z along the series H_2X_2 ($X = O, S, Se, Te, Po$) ($\log(M_{PV}^X)$ vs. $\log(Z)$). The total contribution is split into an atomic integral $\langle ns_{1/2}^X | \gamma_5 \rho^X | np_{1/2}^X \rangle$ weighted by the mixing coefficients of the atomic orbitals in the molecule as in eqn (32).

4.2 Visualization of the electron chirality density in the 4-component relativistic framework

In section 2.2 the reduced contributions

$$M_{PV}^X = \sum_i^{N_{occ}} \langle \psi_i | \gamma_5 \rho^X | \psi_i \rangle \quad (33)$$

have been studied by means of a projection analysis. The integrals M_{PV}^X have been shown to exhibit an intriguing dependence on the H–X–X–H dihedral angle through the changing chiral environment probed at the atomic centers X and in their immediate vicinity by the normalized nuclear charge distribution ρ^X . In this section we wish to visualize this dependence by defining a density $\gamma_5(\mathbf{r})$, such that

$$\int \gamma_5(\mathbf{r}) \rho^X(\mathbf{r}) d\mathbf{r} \equiv \sum_i^{N_{occ}} \langle \psi_i | \gamma_5 \rho^X | \psi_i \rangle. \quad (34)$$

If we consider the atomic centers X fixed in space during the variation of the H–X–X–H dihedral angle (Figure 5) then the geometry dependence of M_{PV}^X is carried by the $\gamma_5(\mathbf{r})$ density alone, whereas the probing $\rho^X(\mathbf{r})$ is independent of the positions of other atoms and therefore independent of the chiral environment created by these centers.

The density $\gamma_5(\mathbf{r})$ has been introduced in the NR framework by Hegstrom^{66,67} under the name electron chirality density, a name which we will adopt also in our work. In the 4-component relativistic theory the density $\gamma_5(\mathbf{r})$ takes a particularly simple form given the structure of the γ_5 Dirac matrix, eqn (10) and can be evaluated in AO basis according to

$$\gamma_5(\mathbf{r}) = \sum_{\kappa\lambda} [\chi_{\kappa}^{\dagger}(\mathbf{r}) \chi_{\lambda}(\mathbf{r}) D_{\lambda\kappa} + \chi_{\lambda}^{\dagger}(\mathbf{r}) \chi_{\kappa}(\mathbf{r}) D_{\kappa\lambda}], \quad (35)$$

where the indices κ and λ map large and small component basis functions χ , respectively, and $D_{\lambda\kappa}$ represents elements of the AO density matrix. In contrast to the NR theory where SO coupling needs to be introduced perturbationally to yield nonzero $\gamma_5(\mathbf{r})$, we can work with the *unperturbed* SCF density matrix since SO coupling is introduced variationally from the start.

The significance of the electron chirality density is the fact that an understanding and modeling of the electron chirality density depending on the molecular building blocks and their relative geometry and orientation would allow to model the PV expectation value. The relationship between $\gamma_5(\mathbf{r})$ and the PV expectation value is particularly simple when using the point charge (PC) nuclear model:

$$E_{PV}^{PC} = \frac{G_F}{2\sqrt{2}} \sum_A Q_w^A \int \gamma_5(\mathbf{r}) \rho^A \delta^3(\mathbf{r} - \mathbf{r}_A) d\mathbf{r} = \frac{G_F}{2\sqrt{2}} \sum_A Q_w^A \gamma_5(\mathbf{r}_A). \quad (36)$$

Using this model, $\gamma_5(\mathbf{r}_A) = M_{PV}^A$, and the PV expectation value is a simple sum of the electron chirality densities evaluated at the atomic centers A and scaled with the respective weak charges Q_w^A and the prefactor $G_F/2\sqrt{2}$ whereas the more realistic Gaussian distribution model for the normalized nuclear charge density ρ^A would require the knowledge of $\gamma_5(\mathbf{r})$ also in the close vicinity of the nuclear center.

It is important to realize that the electron chirality density $\gamma_5(\mathbf{r})$ itself is very atomic in nature. This follows from the very atomic nature of the small components and the fact that the γ_5 matrix, eqn (10), couples the large and the small components of 4-spinors. This feature is illustrated in Figure 6 where we compare the reduced contribution M_{PV}^{Te} and the integrated electron chirality density for H_2Te_2 , both calculated at the HF level, as a function of dihedral angle. The two curves are qualitatively very similar (Figure 6), but only M_{PV}^{Te} is integrated including the nucleon density.

In Figure 7 we have plotted the HF $\gamma_5(\mathbf{r})$ around one Te atom in H_2Te_2 for selected H–Te–Te–H dihedral angles using the orientation sketched in Figure 5. The dimensions of the plots ($0.2 \times 0.2 a_0$) are restricted to the close vicinity of the Te center position since only the nuclear region is significant for the PV expectation value. At all dihedral angles one can observe regions of positive and negative $\gamma_5(\mathbf{r})$ and several contour lines representing isosurfaces where $\gamma_5(\mathbf{r}) = 0$ relatively close to the nucleus. At the dihedral angle 0° $\gamma_5(\mathbf{r})$ has four lobes around the nucleus which lies exactly in the $\gamma_5(\mathbf{r}) = 0$ nodal surface – this corresponds to a zero PV expectation value at this molecular structure (all nuclei lie in the nodal surface and the molecular expectation value is zero). Increasing the dihedral angle from zero, the nodal surface shifts away from the nucleus which enters a region of positive $\gamma_5(\mathbf{r})$ with increasing magnitude and this corresponds to the general behavior of the curves in Figure 1. Close to the 90° dihedral

angle the $\gamma_5(\mathbf{r}) = 0$ nodal surface returns and passes through the nucleus which can then be seen in a region of (relatively small) negative $\gamma_5(\mathbf{r})$ at 105° dihedral angle. At 180° dihedral angle (not shown in Figure 7 because plot would be zero everywhere), all nuclei lie again in the $\gamma_5(\mathbf{r}) = 0$ nodal surface (mirror plane).

In all plots presented in Figure 7 the $\gamma_5(\mathbf{r}) = 0$ nodal surfaces are relatively close to the nuclear center, which illustrates the general difficulty for understanding and modeling the PV expectation value: it is possible to obtain very different atomic contributions E_{PV}^X of even opposite sign by only a tiny displacement of the nodal surface induced by a minute change in the molecular structure.

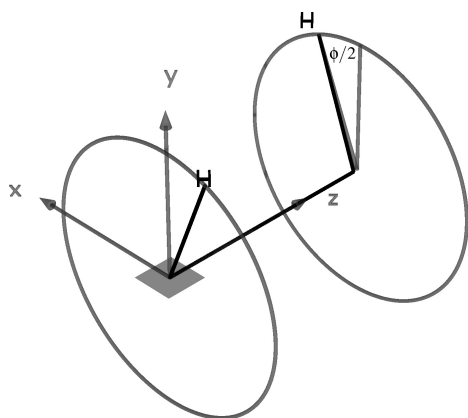


Fig. 5 Orientation of the H_2Te_2 molecule employed in the visualization of the electron chirality density (Figure 7). The dihedral angle H-Te-Te-H is twice the angle between the Te-Te-H plane and the yz plane. The electron chirality density is plotted in the xz plane around one Te atom (gray rectangle; size of this rectangle is not proportional to the bond distances).

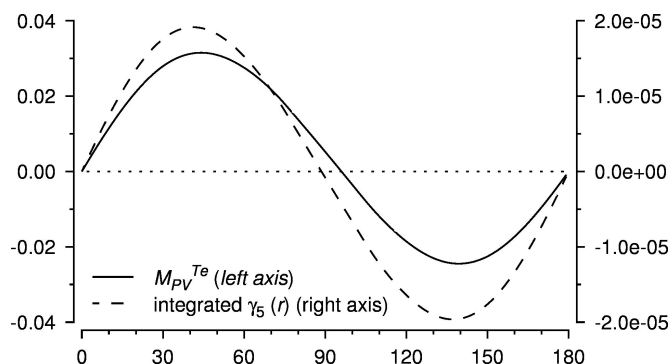


Fig. 6 Reduced HF contribution M_{PV}^{Te} for H_2Te_2 (left axis) and the integrated HF electron chirality density $\gamma_5(\mathbf{r})$, eqn (35), (right axis) as a function of dihedral angle (both in atomic units).

4.3 A variational approach to the single-center theorem

In contrast to the hydrogen dichalcogenides, the CHBrClF molecule has been subject to experimental studies of PV in molecules, albeit so far with negative result. Following a suggestion by Letokhov and co-workers,^{119,120} the group of Chardonnet searched for the signature of parity violation in the CHBrClF molecule in the form of a difference $\Delta v_{PV} = v_{R(-)} - v_{S(+)}$ between the two enantiomers in their infrared spectral absorption line frequencies. More precisely a hyperfine component of the C-F stretching fundamental was probed by laser-saturated absorption spectroscopy.^{30,121} In these experiments a sensitivity $\Delta v_{PV}/v$ of 5×10^{-14} was attained. However, theoretical calculations indicate that the PV shift $\Delta v_{PV}^{0 \rightarrow 1}$ for the fundamental $0 \rightarrow 1$ transition of the C-F stretch of CHBrClF is on the order of -2.4 mHz,^{56,122-124} corresponding to $\Delta v_{PV}/v \approx -8 \times 10^{-17}$, that is, three orders of magnitude smaller. In view of these results, the group of Chardonnet has oriented their research towards molecules containing heavier atoms, such as oxorhenium compounds, and are developing a new ultra-high resolution experiment based on the sub-Doppler two-photon Ramsey fringes technique which targets a sensitivity of 0.01 Hz (3×10^{-16}) or better.^{35,57,60}

The PV shift of the fundamental C-F stretching mode of the CHBrClF molecule has been calculated both as an expectation value, eqn (14), in a 4-component relativistic framework^{56,105,125} and as a linear response function, eqn (16), in a NR framework.^{122,126,127} In the latter case the PV energy is expressed as a double sum involving the NR PV Hamiltonian and SO operators associated with the constituent atoms of the molecule. Diagonal terms are zero according to the single-center theorem of Hegstrom *et al.*³⁷ In this section we explore a hybrid approach which allows us to probe the single-center theorem in a variational framework. We perform 2-component relativistic calculations based on the X2C Hamiltonian. In such calculations an exact block diagonalization of the parent Dirac Hamiltonian to 2-component form is carried out. The corresponding picture transformation of the two-electron operator is not carried out, since the resulting two-electron integrals are expressed in terms of the full set of two-electron integrals of the 4-component calculation and thus engenders a computational cost *higher* than the parent calculation. Instead, two-electron SO contributions are typically generated in an atomic mean-field fashion, in our case by the AMFI code.^{102,103} We have carried out a series of calculations in which the X2C Hamiltonian in the spinfree form has been combined with both one- and two-electron SO contributions generated by the AMFI code for a single atom at a time. The PV energy is then calculated as an expectation value, but with a wave function generated with SO contributions from a single center. A similar approach has been employed by van Wüllen in a computational study of magnetic anisotropy.¹²⁸ We also

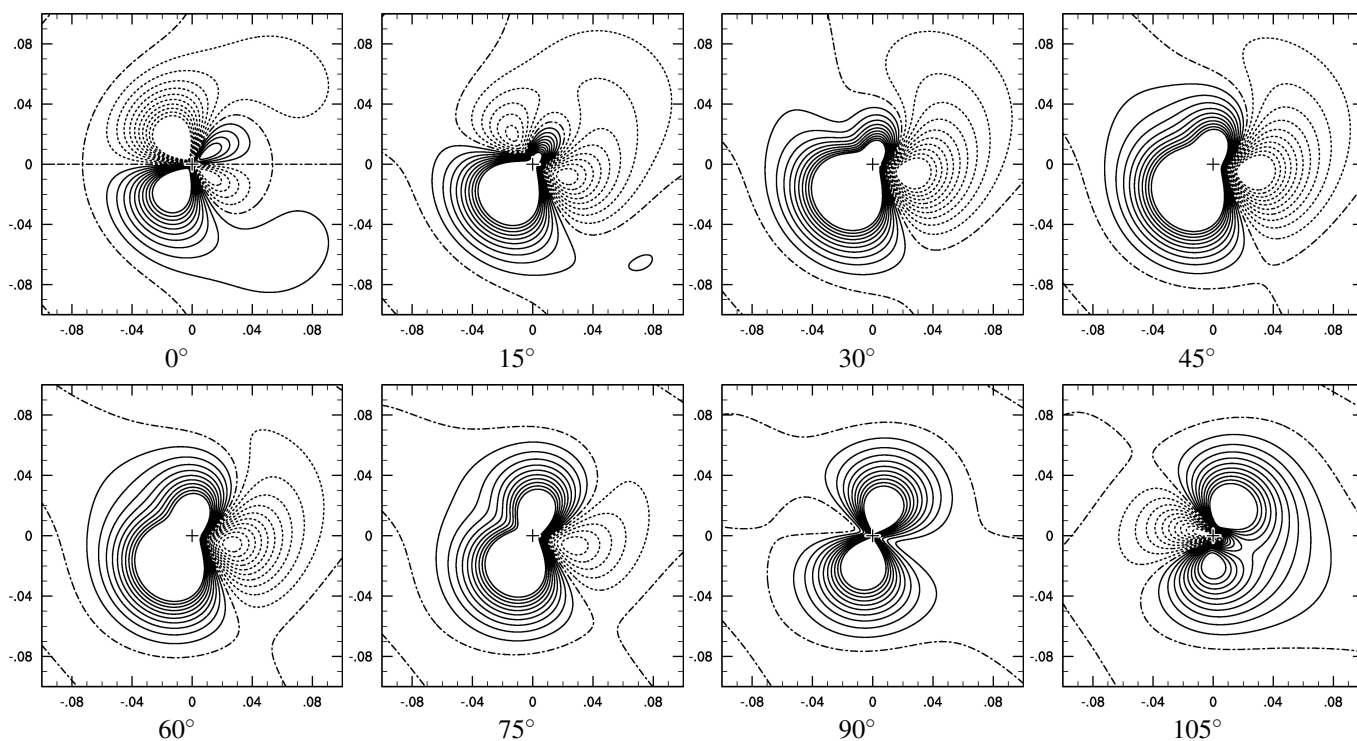


Fig. 7 HF electron chirality density $\gamma_5(\mathbf{r})$, eqn (35), around one Te atom in H_2Te_2 for several H-Te-Te-H dihedral angles (for the orientation of the molecule, see Figure 5). Solid (dotted) contour lines are plotted in the range from $+0.0005$ to $+0.005$ (-0.0005 to -0.005) atomic units in intervals of 0.0005 atomic units. The dash-dotted contour line represents $\gamma_5(\mathbf{r}) = 0$. The cross represents the position of the nucleus. The dimensions of the plots are $0.2 \times 0.2 a_0$.

note in passing that a 2-component Zeroth-Order Regular Approximation (ZORA) study of molecular parity violation has been reported by Berger et al.¹²⁹

The resulting PV energies E_{PV} at the equilibrium geometry of CHBrClF are given in Table 5. For comparison we also give corresponding values obtained from conventional calculations based on the 2-component X2C and the 4-component DC Hamiltonian. In all calculations we employ a point charge model for the nuclei, which, in view of the discussion in section 2.2, implies that contributions to E_{PV} are exclusively obtained from mixing of atomic $s_{1/2}$ and $p_{1/2}$ orbitals on the same center and thus conforms to the restriction imposed on the single-center theorem.³⁷ The entries of the first five columns of Table 5 are given in the form $(A_{\text{PV}}, B_{\text{SO}})$ where the row refers to the atomic contribution E_{PV}^A to the total PV energy and the column to the SO-active nucleus. The individual PV contributions are summed up in column six and, comparing to the results obtained by conventional X2C calculations in column seven, one indeed observes a high degree of additivity of the individual SO-contributions, as implied by the structure of eqn (16). We also note a very good agreement of the 2-component X2C results with the full 4-component DC

results, with a maximum deviation of 4% for the bromine PV contribution, in agreement with previous observations in refs. 57 and 130. However, the diagonal elements of Table 5 are generally *not* zero, and even quite significantly so for the heavier elements. This is contrary to the single-center theorem and may indicate significant higher-order SO contributions. We also note that the individual PV contributions from the Br and Cl atoms have opposite signs and so the presence of two heavy atoms have a destructive, rather than constructive effect.

In Table 6 we give the corresponding PV shifts associated with the fundamental C–F stretch of the CHBrClF molecule. Again we observe strong additivity of individual atomic SO-contributions and good agreement with both conventional 2-component X2C results as well as 4-component DC results. We note that both the PV- and SO-contributions from the Br and Cl atoms come with opposite signs. In Table 6 we also give the purely harmonic contributions to the PV shift, showing that all atomic PV contributions change sign when anharmonicity is taken into account, emphasizing the importance of including this effect into simulations of the PV shift in molecular vibrational spectra.¹²⁵

Table 5 Contributions to the parity violating energy E_{PV} for the CHBrClF molecule. The first five columns give the E_{PV} contributions with only one spin-orbit active nucleus, summed up in column six, labelled “Sum”. In these calculations both one- and two-electron SO-contributions were provided by the AMFI module. The final two columns refer to calculations based on the conventional X2C Hamiltonian and the 4-component Dirac-Coulomb (DC) Hamiltonian, respectively. A point nucleus model was employed in these calculations. All values in $10^{-18}E_h$

	C	H	F	Br	Cl	Sum	X2C	DC
C	-0.0001	0.0000	-0.0028	0.0594	0.0010	0.0576	0.0574	0.0575
H	0.0000	0.0000	0.0000	0.0000	0.0000	0.0000	0.0000	0.0000
F	-0.0035	0.0000	0.0008	1.0719	-0.1868	0.8823	0.8735	0.8798
Br	-0.6097	0.0007	1.9386	2.4255	4.7602	8.5153	7.8545	8.2086
Cl	0.0584	0.0007	-0.1048	-3.4845	-0.0590	-3.5893	-3.5330	-3.5986
Sum	-0.5550	0.0015	1.8318	0.0724	4.5154	5.8660	5.2524	5.5473

5 Conclusion

In this contribution we have analyzed parity violation in sample chiral molecules in a 2- and 4-component relativistic framework. Spin-orbit interaction is accordingly included variationally, and the parity violation energy E_{PV} may be calculated as an expectation value, eqn (14). We have carried out a decomposition of the molecular expectation value in atomic contributions and demonstrate that E_{PV} is completely dominated by intra-atomic contributions. By integrating the electron chirality density $\gamma_5(\mathbf{r})$ we show that the atomic nature of parity violation arises not only from the presence of nuclear charge densities in the weak interaction Hamiltonian, but also from the coupling of the large and small components of Dirac 4-spinors by the γ_5 matrix. The interaction Hamiltonian samples the electron chirality density in nuclear regions, and we show that the nodal structure of $\gamma_5(\mathbf{r})$, and thus its sign in nuclear regions, is quite sensitive to molecular structure.

The picture which emerges from our analysis is that the parity violating energy arises from the mixing of valence $s_{1/2}$ and $p_{1/2}$ atomic orbitals on the same center, induced by a chiral molecular field. This picture contrasts with the manifestly inter-atomic mechanism suggested by the non-relativistic framework in which the parity violation energy is calculated as a linear response function, eqn (16). We have carried out 2-component relativistic calculations on the CHBrClF molecule in which only one nucleus is spin-orbit active at a time and demonstrate that the spin-orbit contributions are indeed to a large extent additive, giving PV energies and vibrational shifts in good agreement with both conventional 2-component X2C results as well as 4-component DC results. On the other hand, we show that for the heaviest atom bromine the spin-orbit contribution gives a significant contribution to the parity violation energy of the same center contrary to the single-center theorem. We attribute this result to higher-order spin-orbit effects not taken into account by the single-center

theorem.

The intra-atomic picture of parity violation that emerges from our analysis in a relativistic framework, summarized by eqn (32), suggests that it may be possible to construct a model for parity violation in chiral molecules by combining pre-calculated atomic quantities by simple bonding models, the latter providing estimates for the mixing of $s_{1/2}$ and $p_{1/2}$ atomic orbitals in the molecular field. Such a model would not only allow a rapid scan of candidate molecules for experiment, but may ultimately allow the *in silico* design of such molecules.

6 Acknowledgment

This work is part of the project NCP-CHEM funded by the Agence Nationale de la Recherche (ANR, France). A.S.P.G. acknowledges postdoc funding from the ANR under the NCP-MOL project. P.S. was supported by the Marsden Fund Council (Contract No. MAU0606) from Government funding administered by the Royal Society of New Zealand. R.B. has received support from the Norwegian Research Council through a Centre of Excellence Grant (Grant No. 179568/V30). L.V. was supported by the Netherlands Organization for Scientific Research (NWO) via a Vici grant. M.I. was supported by the Grant Agency of the Slovak Republic (Grant No. VEGA-1/0356/09 and VEGA-1/0520/10), as well as a postdoc grant from the French Ministry of Science and Technology.

Table 6 Contributions to the parity violating transition frequency difference $\Delta\nu_{\text{pv}}^{0\rightarrow 1}$ between the two enantiomers (R-S) for the fundamental $0 \rightarrow 1$ transition of the C–F stretching mode of the CHBrClF molecule. The first five columns give the contributions with only one spin-orbit active nucleus, summed up in column six, labelled “Sum”. In these calculations both one- and two-electron SO-contributions were provided by the AMFI module. The next two columns refer to calculations based on the conventional X2C Hamiltonian and the 4-component Dirac-Coulomb (DC) Hamiltonian, respectively, whereas the final column reports the harmonic contribution to the DC calculation. A point nucleus model was employed in these calculations. All values in mHz

	C	H	F	Br	Cl	Sum	X2C	DC	DC ^{harm}
C	0.000	0.000	0.001	0.172	−0.041	0.132	0.132	0.132	−0.027
H	0.000	0.000	0.000	0.000	0.000	0.000	0.000	0.000	0.000
F	0.000	0.000	0.000	−0.043	−0.001	−0.044	−0.047	−0.046	0.100
Br	0.285	−0.003	0.066	−1.175	−2.518	−3.345	−3.355	−3.334	2.309
Cl	−0.018	0.000	−0.013	1.424	0.013	1.406	1.408	1.412	−0.349
Sum	0.267	−0.003	0.054	0.378	−2.547	−1.851	−1.862	−1.836	2.060

References

- H. Kunz, *Angew. Chem. Int. Ed.*, 2008, **41**, 4439–4451.
- S. F. Mason, *Int. Rev. Phys. Chem.*, 1983, **3**, 217–241.
- J. Gal, *Chirality*, 2010, DOI: 10.1002/chir.20866.
- U. Meyerhenrich, *Amino Acids and the Asymmetry of Life*, Springer, Heidelberg, 2008.
- W. G. Armstrong, L. B. Halstead, F. B. Reed and L. Wood, *Phil. Trans. Royal Soc. (London)*, 1983, **301**, 301–343.
- W. A. Bonner, *Top. Stereochem.*, 1988, **18**, 1.
- W. A. Bonner, *Orig. Life Evol. Biospheres*, 1991, **21**, 59–111.
- H. Buschmann, R. Thede and D. Heller, *Angew. Chem. Int. Ed.*, 2000, **39**, 4033–4036.
- W. A. Bonner, *Orig. Life Evol. Biospheres*, 1995, **25**, 175–190.
- W. A. Bonner, *Chirality*, 2000, **12**, 114–126.
- R. N. Compton and R. M. Pagni, *Adv. At. Mol. Opt. Phys.*, 2002, **48**, 219–261.
- P. Schwerdtfeger and U. Müller-Herold, in *Symmetry 2000, Vol. 1*, Portland Press, London, 2002, ch. From Symmetry to Asymmetry – Electroweak Parity Violation and Biomolecular Homochirality, p. 317.
- H. Urata, H. Shimizu, H. Hiroaki, D. Kohda and M. Akagi, *Biochem. Biophys. Res. Commun.*, 2003, **309**, 79–83.
- H. Urata and M. Akagi, *Tetrahedron Lett.*, 1996, **37**, 5551–5554.
- H. Urata, M. Go and H. H. M. Akagi, *Nucleic Acid Res. Suppl.*, 2003, **3**, 41–42.
- A. K. Ryan, B. Blumberg, C. R.-E. S. Yonei-Tamura, K. Tamura, T. Tsukui, J. de la Pena, W. Sabbagh, J. Greenwald, S. Choe, D. P. Norris, E. J. Robertson, R. M. Evans, M. G. Rosenfeld and J. C. I. Belmonte, *Nature*, 1998, **394**, 545–551.
- R. A. Hegstrom and D. K. Kondepudi, *Sci. Am.*, 1990, **262**, 108–115.
- C. Wu, E. Ambler, R. Hayward, D. Hoppes and R. Hudson, *Phys. Rev.*, 1957, **105**, 1413–1415.
- T. Lee and C. Yang, *Phys. Rev.*, 1956, **104**, 254–258.
- S. L. Glashow, *Rev. Mod. Phys.*, 1980, **52**, 539–543.
- S. Weinberg, *Phys. Rev. Lett.*, 1967, **19**, 1264–1266.
- A. Salam, in *Elementary Particle Theory, Relativistic Groups, and Analyticity*, Proceedings of the 8th Nobel Symposium, Almqvist and Wiksells, Stockholm, 1968, ch. Weak and Electromagnetic Interactions, p. 367.
- A. Salam, in *Chemical Evolution: Origin of Life*, ed. C. Ponnampereuma and J. Chela-Flores, A Deepak Publishing, Hampton, Virginia, USA, 1993, ch. The Origin of Chirality, the Role of Phase Transitions and Their Inductions in Amino Acids, pp. 101–117.
- C. S. Wood, S. C. Bennett, D. Cho, B. P. Masterson, J. L. Roberts, C. E. Tanner and C. E. Wieman, *Science*, 1997, **275**, 1759–1763.
- C. S. Wood, S. C. Bennett, J. L. Roberts, D. Cho and C. E. Wieman, *Can. J. Phys.*, 1999, **77**, 7–75.
- S. G. Porsev, K. Beloy and A. Derevianko, *Phys. Rev. Lett.*, 2009, **102**, 181601.
- V. A. Dzuba, V. V. Flambaum and J. S. M. Ginges, *Phys. Rev. D*, 2002, **66**, 076013.
- B. Y. Zel’dovich, D. B. Saakyan and I. I. Sobel’man, *JETP Lett.*, 1977, **25**, 94–97.
- D. W. Rein, R. A. Hegstrom and P. G. H. Sandars, *Phys. Lett. A*, 1979, **71**, 499–502.
- C. Daussy, T. Marrel, A. Amy-Klein, C. T. Nguyen, C. J. Bordé and C. Chardonnet, *Phys. Rev. Lett.*, 1999, **83**, 1554–1557.
- A. S. Lahamer, S. M. Mahurin, R. N. Compton, D. House, J. K. Laerdahl, M. Lein and P. Schwerdtfeger, *Phys. Rev. Lett.*, 2000, **85**, 4470–4473.
- R. Berger, in *Parity-violation effects in molecules*, in: P. Schwerdtfeger (Ed.), *Relativistic Electronic Structure Theory, Part 2, Applications*, Elsevier, Netherlands, 2004, pp. 188–288.
- M. Quack, J. Stohner and M. Willeke, *Annu. Rev. Phys. Chem.*, 2008, **59**, 741–769.
- P. Schwerdtfeger, in *Computational Spectroscopy*, Wiley-VCH, Weinheim, 2010, ch. The Search for Parity Violation in Chiral Molecules, p. 201.
- B. Darquié, C. Stoeffler, S. Zrig, J. Crassous, P. Soullard, P. Asselin, T. R. Huet, L. Guy, R. Bast, T. Saue, P. Schwerdtfeger, A. Shelkovnikov, C. Daussy, A. Amy-Klein and C. Chardonnet, *Chirality*, 2010, **22**, 870.
- Y. Yamagata, *J. Theoret. Biol.*, 1966, **11**, 495–498.
- R. A. Hegstrom, D. W. Rein and P. G. H. Sandars, *J. Chem. Phys.*, 1980, **73**, 2329–2341.
- S. F. Mason and G. E. Tranter, *Chem. Phys. Lett.*, 1983, **94**, 34–37.
- S. F. Mason and G. E. Tranter, *Chem. Commun.*, 1983, 117–119.
- S. F. Mason and G. E. Tranter, *Mol. Phys.*, 1984, **397**, 1091–1111.
- G. E. Tranter, *Chem. Phys. Lett.*, 1985, **115**, 286–290.
- G. E. Tranter, *Chem. Phys. Lett.*, 1985, **121**, 339–342.
- G. E. Tranter, *Chem. Phys. Lett.*, 1987, **135**, 279–282.
- A. J. McDermott and G. E. Tranter, *Chem. Phys. Lett.*, 1992, **194**, 152–156.
- A. J. McDermott, *Orig. Life Evol. Biospheres*, 1995, **25**, 191–199.
- S. F. Mason, *Nature*, 1984, **311**, 19–23.
- M. Quack, *Angew. Chem. Int. Ed.*, 1989, **28**, 571–586.
- S. F. Mason and G. E. Tranter, *Proc. Roy. Soc. Lond. A*, 1985, **397**, 45–65.
- R. Wesendrup, J. K. Laerdahl, R. N. Compton and P. Schwerdtfeger, *J.*

- Phys. Chem. A*, 2003, **107**, 6668–6673.
- 50 R. Berger and M. Quack, *ChemPhysChem*, 2000, **1**, 57–60.
- 51 J. K. Laerdahl, R. Wesendrup and P. Schwerdtfeger, *ChemPhysChem*, 2000, **1**, 60–62.
- 52 P. Lazzarotti and R. Zanasi, *Chem. Phys. Lett.*, 1997, **279**, 349–354.
- 53 A. Bakasov, T.-K. Ha and M. Quack, *J. Chem. Phys.*, 1998, **109**, 7263–7285.
- 54 R. Berger and M. Quack, *J. Chem. Phys.*, 2000, **112**, 3148–3158.
- 55 A. C. Hennum, T. Helgaker and W. Klopper, *Chem. Phys. Lett.*, 2002, **354**, 274–282.
- 56 P. Schwerdtfeger, T. Saue, J. N. P. van Stralen and L. Visscher, *Phys. Rev. A*, 2005, **71**, 012103.
- 57 F. D. Montigny, R. Bast, A. S. P. Gomes, G. Pilet, N. Vanthuyne, C. Roussel, L. Guy, P. Schwerdtfeger, T. Saue and J. Crassous, *Phys. Chem. Chem. Phys.*, 2010, **12**, 8792–8803.
- 58 R. Sullivan, M. Pyda, J. Pak, B. Wunderlich, J. R. Thompson, R. Pagni, H. Pan, C. Barnes, P. Schwerdtfeger and R. Compton, *J. Phys. Chem. A*, 2003, **107**, 6674–6680.
- 59 M. Quack, *Angew. Chem. Int. Ed.*, 2002, **41**, 4618–4630.
- 60 J. Crassous, F. Monier, J.-P. Dutasta, M. Ziskind, C. Daussy, C. Gain and C. Chardonnet, *ChemPhysChem*, 2003, **4**, 541–548.
- 61 J. Crassous, C. Chardonnet, T. Saue and P. Schwerdtfeger, *Org. Biomol. Chem.*, 2005, **12**, 2218–2224.
- 62 R. A. Harris and L. Stodolsky, *Phys. Lett. B*, 1978, **78**, 313–317.
- 63 J. K. Laerdahl and P. Schwerdtfeger, *Phys. Rev. A*, 1999, **60**, 4439–4453.
- 64 S. Nahrwold and R. Berger, *J. Chem. Phys.*, 2009, **130**, 214101.
- 65 F. Faglioni and P. Lazzarotti, *Phys. Rev. E*, 2002, **65**, 011904.
- 66 R. A. Hegstrom, J. P. Chamberlain, K. Seto and R. G. Watson, *Am. J. Phys.*, 1988, **56**, 1086–1092.
- 67 R. Hegstrom, *J. Mol. Struct. (Theochem)*, 1991, **232**, 17–21.
- 68 M. A. Bouchiat and C. Bouchiat, *J. Physique*, 1974, **35**, 899–927.
- 69 F. Halzen and A. D. Martin, *Quarks & Leptons*, John Wiley, New York, 1984.
- 70 W. Greiner, and B. Müller, *Gauge Theory of Weak Interactions*, Springer, 2009.
- 71 K. Schwarzschild, *Gött. nach. Math.-Phys. Kl.*, 1903, 126–131.
- 72 J. J. Sakurai, *Advanced Quantum Mechanics*, Addison-Wesley, Reading, Massachusetts, 1967.
- 73 E. Fermi, *Zeit. Phys.*, 1934, **88**, 161–177.
- 74 F. L. Wilson, *Am. J. Phys.*, 1968, **36**, 1150–1160.
- 75 K. Nakamura, *et al.*, *J. Phys. G*, 2010, **37**, 075021.
- 76 P. L. Anthony, R. G. Arnold, C. Arroyo, K. Bega, J. Biesiada, P. E. Bosted, G. Bower, J. Cahoon, R. Carr, G. D. Cates, J.-P. Chen, E. Chudakov, M. Cooke, P. Decowski, A. Deur, W. Emam, R. Erickson, T. Fieguth, C. Field, J. Gao, M. Gary, K. Gustafsson, R. S. Hicks, R. Holmes, E. W. Hughes, T. B. Humensky and G. M. Jones, *Phys. Rev. Lett.*, 2005, **95**, 081601.
- 77 A. L. Barra, J.-B. Robert and L. Wiesenfeld, *Phys. Lett. A*, 1986, **115**, 443–447.
- 78 A. L. Barra, J.-B. Robert and L. Wiesenfeld, *Europhys. Lett.*, 1988, **5**, 217–222.
- 79 A. L. Barra and J.-B. Robert, *Mol. Phys.*, 1996, **88**, 875–886.
- 80 G. Laubender and R. Berger, *ChemPhysChem*, 2003, **4**, 395–399.
- 81 A. Soncini, F. Faglioni and P. Lazzarotti, *Phys. Rev. A*, 2003, **68**, 033402.
- 82 V. Weijo, P. Manninen and J. Vaara, *J. Chem. Phys.*, 2005, **123**, 054501.
- 83 R. Bast, T. Saue and P. Schwerdtfeger, *J. Chem. Phys.*, 2006, **125**, 064504.
- 84 G. Laubender and R. Berger, *Phys. Rev. A*, 2006, **74**, 032105.
- 85 V. Weijo, R. Bast, P. Manninen, T. Saue and J. Vaara, *J. Chem. Phys.*, 2007, **126**, 074107.
- 86 V. Weijo, P. Manninen and J. Vaara, *Theor. Chem. Acc.*, 2008, **121**, 53–57.
- 87 V. Weijo, M. B. Hansen, O. Christiansen and P. Manninen, *Chem. Phys. Lett.*, 2009, **470**, 166–171.
- 88 C. H. Townes and B. P. Dailey, *J. Chem. Phys.*, 1949, **17**, 782–796.
- 89 S. Dubillard, J.-B. Rota, T. Saue and K. Fægri, *J. Chem. Phys.*, 2007, **124**, 154307.
- 90 DIRAC, a relativistic ab initio electronic structure program, Release DIRAC08 (2008), written by L. Visscher, H. J. Aa. Jensen, and T. Saue, with new contributions from R. Bast, S. Dubillard, K. G. Dyall, U. Ekström, E. Eliav, T. Fleig, A. S. P. Gomes, T. U. Helgaker, J. Henriksson, M. Iliaš, Ch. R. Jacob, S. Knecht, P. Norman, J. Olsen, M. Pernpointner, K. Ruud, P. Salek, and J. Sikkema (see <http://dirac.chem.sdu.dk>).
- 91 J. C. Slater, *Phys. Rev.*, 1951, **81**, 385–390.
- 92 S. J. Vosko, L. Wilk and M. Nusair, *Can. J. Phys.*, 1980, **58**, 1200–1211.
- 93 A. D. Becke, *Phys. Rev. A*, 1988, **38**, 3098–3100.
- 94 C. Lee, W. Yang and R. G. Parr, *Phys. Rev. B*, 1988, **37**, 785–789.
- 95 B. Miehlich, A. Savin, H. Stoll and H. Preuss, *Chem. Phys. Lett.*, 1989, **157**, 200–206.
- 96 P. J. Stephens, F. J. Devlin, C. F. Chabalowski and M. J. Frisch, *J. Phys. Chem.*, 1994, **98**, 11623–11627.
- 97 A. D. Becke, *J. Chem. Phys.*, 1993, **98**, 5648–5652.
- 98 J. P. Perdew and K. Schmidt, *Density Functional Theory and Its Applications to Materials*, American Institute of Physics, Melville, 2001, vol. 577, pp. 1–20.
- 99 L. Visscher and T. Saue, *J. Chem. Phys.*, 2000, **113**, 3996–4002.
- 100 L. Visscher, *Theor. Chem. Acc.*, 1997, **98**, 68–70.
- 101 M. Iliaš and T. Saue, *J. Chem. Phys.*, 2007, **126**, 064102.
- 102 B. Schimmelpfennig, 1996, program AMFI, Stockholm, Sweden.
- 103 B. A. Hess, C. M. Marian, U. Wahlgren and O. Gropen, *Chem. Phys. Lett.*, 1996, **251**, 365–371.
- 104 M. Iliaš, V. Kellö, L. Visscher and B. Schimmelpfennig, *J. Chem. Phys.*, 2001, **115**, 9667–9674.
- 105 P. Schwerdtfeger, J. K. Laerdahl and C. Chardonnet, *Phys. Rev. A*, 2002, **65**, 042508.
- 106 L. Visscher and K. G. Dyall, *At. Data Nucl. Data Tables*, 1997, **67**, 207–224.
- 107 A. Bakasov and M. Quack, *Chem. Phys. Lett.*, 1999, **303**, 547–557.
- 108 R. Berger and C. van Wüllen, *J. Chem. Phys.*, 2005, **122**, 134316.
- 109 K. Ruud and T. Helgaker, *Chem. Phys. Lett.*, 2002, **352**, 533–539.
- 110 N. Weinberg and K. Mislow, *Can. J. Phys.*, 2000, **78**, 41–45.
- 111 G. Millar, N. Weinberg and K. Mislow, *Mol. Phys.*, 2005, **103**, 2769–2772.
- 112 H. M. Quiney, J. K. Laerdahl, K. Fægri and T. Saue, *Phys. Rev. A*, 1998, **57**, 920.
- 113 K. G. Dyall and K. Fægri, *Introduction to Relativistic Quantum Chemistry*, Oxford University Press, 2007.
- 114 I. B. Khriplovich, *Parity nonconservation in atomic phenomena*, Gordon and Breach Science Publishers, Philadelphia, 1991.
- 115 I. B. Khriplovich, *Sov. Phys. JETP*, 1980, **52**, 177–180.
- 116 C. S. Wood, S. C. Bennett, D. Cho, B. P. Masterson, J. L. Roberts, C. E. Tanner and C. E. Wieman, *Science*, 1997, **275**, 1759.
- 117 S. C. Bennett and C. E. Wieman, *Phys. Rev. Lett.*, 1999, **82**, 2484–2487.
- 118 T. Saue and H. J. A. Jensen, *J. Chem. Phys.*, 1999, **111**, 6211–6222.
- 119 V. S. Letokhov, *Phys. Lett. A*, 1975, **54**, 275–276.
- 120 O. N. Kompanets, A. R. Kukudzhanov, L. L. Gervits and V. S. Letokhov, *Opt. Commun.*, 1976, **19**, 414–416.
- 121 M. Ziskind, T. Marrel, C. Daussy and C. Chardonnet, *Eur. Phys. J. D*, 2002, **20**, 219–225.
- 122 M. Quack and J. Stohner, *J. Chem. Phys.*, 2003, **119**, 11228–11240.
- 123 G. Rauhut, V. Barone and P. Schwerdtfeger, *J. Chem. Phys.*, 2006, **125**, 054308.

-
- 124 R. Berger and J. L. Stuber, *Mol. Phys.*, 2007, **105**, 41–49.
- 125 J. K. Laerdahl, P. Schwerdtfeger and H. M. Quiney, *Phys. Rev. Lett.*, 2000, **84**, 3811–3814.
- 126 M. Quack and J. Stohner, *Phys. Rev. Lett.*, 2000, **84**, 3807–3810.
- 127 R. G. Vignione, R. Zanasi, P. Lazzeretti and A. Ligabue, *Phys. Rev. A*, 2000, **62**, 052516.
- 128 C. van Wüllen, *J. Chem. Phys.*, 2009, **130**, 194109.
- 129 R. Berger, N. Langermann and C. van Wüllen, *Phys. Rev. A*, 2005, **71**, 042105.
- 130 D. Figgen, T. Saue and P. Schwerdtfeger, *J. Chem. Phys.*, 2010, **132**, 234310.